HHS Public Access

Author manuscript

Shock. Author manuscript; available in PMC 2021 October 01.

Published in final edited form as:

Shock. 2020 October ; 54(4): 539–547. doi:10.1097/SHK.0000000000001516.

Inhibition of PAR-2 attenuates neuroinflammation and improves short-term neurocognitive functions via ERK1/2 signaling following asphyxia-induced cardiac arrest in rats

Umut Ocak[1,2,3], **Pinar Eser Ocak**[1,4], **Lei Huang**[1,5], **Gang Zuo**[1,6], **Jun Yan**[1,7], **Xin Hu**[1,8], **Zhijun Song**[1,9], **John H. Zhang**[1,5,10,11]

[1]Department of Physiology and Pharmacology, Loma Linda University School of Medicine, Loma Linda, CA 92350, USA

[2]Department of Emergency Medicine, Bursa Yuksek Ihtisas Training and Research Hospital, University of Health Sciences, Bursa 16310, Turkey

[3]Department of Emergency Medicine, Bursa City Hospital, Bursa 16110, Turkey

[4]Department of Neurosurgery, Uludag University School of Medicine, Bursa 16059, Turkey

[5]Department of Neurosurgery, Loma Linda University School of Medicine, Loma Linda, CA 92350, USA

[6]Department of Neurosurgery, The Affiliated Taicang Hospital, Soochow University, Taicang Suzhou, Jiangsu 215400, China

[7]Department of Neurosurgery, The Affiliated Tumor Hospital of Guangxi Medical University, Nanning, Guangxi 530021, China

[8]Department of Neurosurgery, West China Hospital of Sichuan University, Chengdu 610041, China

[9]Department of Neurosurgery, Xingtai Third Hospital, Xingtai, Hebei, 054000, China

[10]Department of Anesthesiology, Loma Linda University School of Medicine, Loma Linda, CA 92350, USA

[11]Department of Neurology, Loma Linda University School of Medicine, Loma Linda, CA 92350, USA

Abstract

Objective—Global cerebral ischemia induced neuroinflammation causes neurofunctional impairment following cardiac arrest. Previous studies have demonstrated that the activation of protease activated receptor-2 (PAR-2) contributes to neuroinflammation. In the present study, we

Corresponding Author: John H. Zhang, MD, PhD, Director, Center for Neuroscience Research, Professor of Anesthesiology, Neurology, Neurosurgery and Physiology, Physiology Program Director, Loma Linda University School of Medicine, Loma Linda, CA 92350, USA, Tel: 909 558-4723 Fax: 909 558-0119, johnzhang3910@yahoo.com.

Declaration of interest statement

The authors report no declarations of interest.

aimed to determine the potential treatment effect of PAR-2 inhibition against neuroinflammation in the setting of asphyxial CA (ACA) in rats.

Methods—A total of 116 adult, male Sprague-Dawley rats were randomly divided into Sham (n= 18) and ACA (n= 98) groups. Time course, short-term outcome and mechanism studies were conducted. All drugs were delivered intranasally. The effect of PAR-2 inhibitor FSLLRY-NH2 on neurocognitive functions was assessed by neurologic deficit score, number of seizures and T-maze test while hippocampal neuronal degeneration was evaluated by Fluoro-Jade C staining after ACA. Western blotting was performed for the mechanism study at 24 hours following ACA. Selective PAR-2 agonist (AC55541) and ERK1/2 inhibitor (PD98059) were used for intervention.

Results—Inhibition of PAR-2 decreased neuroinflammation, reduced the number of degenerating hippocampal neurons and improved neurocognitive functions following ACA. PAR-2 activator alone exerted opposite effects to PAR-2 inhibitor. PAR-2 mediated the augmented brain levels of proinflammatory cytokines by promoting the phosphorylation of ERK1/2.

Conclusions—PAR-2 inhibition diminished neuroinflammation and thereby reduced hippocampal neuronal degeneration and neurocognitive impairment following ACA. This effect was at least partly mediated via the PAR-2/ERK1/2 signaling.

Keywords

cardiac arrest; global cerebral ischemia; neurocognitive; neuroinflammation; protease activated receptor 2

Introduction

Sudden cardiac arrest (CA) is the leading cause of death and an important cause of disability worldwide (1). Besides the low overall survival rate, substantial numbers of CA survivors suffer from moderate to severe functional impairments at hospital discharge. This has long been attributed to the cerebral ischemia/reperfusion (I/R) injury following initial global cerebral ischemia (GCI) and the return of spontaneous circulation (ROSC) (2). Resultantly, injury mechanisms triggered by I/R injury lead to neurofunctional impairment and unfavorable outcomes in CA survivors (3).

Specifically, CA induced GCI has detrimental effects on the ischemia vulnerable brain regions, such as the hippocampus, thalamus, and cerebellum (4–6), depending on the duration of the CA-related ischemic episode (7). Cerebral ischemia is also associated with the activation of microglia and astrocytes which play an important role in neuroinflammatory responses (8, 9) and contribute to hippocampal neuronal degeneration (10). Eventually, neuronal degeneration within the hippocampus, particularly the CA1 region results in neurocognitive impairment following CA (11). The neurocognitive decline, including both short- and long-term memory deficits, depression and apathy (12, 13) may persist up to 3 years after CA and substantially decreases the quality of life of the patients (14).

Protease activated receptor-2 (PAR-2) is a member of the PAR family that is widely expressed in the central nervous system (15, 16). PAR-2 is known as the endogenous

receptor for tryptase (17), the major secretory protein released from mast cells upon their activation and degranulation. The activation of mast cells plays a critical role in the regulation of neuroinflammation (18), as they are capable of initiating, maintaining and magnifying the neuroinflammatory reactions in response to a variety of external stimuli (18, 19). Tryptase was previously shown to potentiate the release of proinflammatory cytokines by activating microglia and astrocytes through PAR-2 *in-vitro* (20, 21). Consistently, we have recently demonstrated that CA was associated with the activation and degranulation of cerebral mast cells and resulted in increased levels of brain tryptase in rats (unpublished data). Importantly, tryptase induced the release of proinflammatory cytokines and this neuroinflammatory response was mediated by PAR-2 in the brains of resuscitated rats.

Tryptase mediated neuroinflammatory response was also associated with the activation of mitogen-activated protein kinases (MAPK) through PAR-2 in earlier studies (15, 20). ERK1/2 is a member of the MAPK, which was previously shown to be activated following reperfusion in both focal ischemia (22) and GCI (23). Interestingly, inhibition of ERK1/2 phosphorylation resulted in better neurologic outcomes as well as improved survival in rodent models of ACA (24).

Based on this background, in the current study, we hypothesized that inhibition of PAR-2 could attenuate neuroinflammation and hippocampal neuronal degeneration, thereby improving short-term neurocognitive functions following asphyxia-induced CA in rats.

Material and Methods

Animals and Asphyxial Cardiac Arrest Rat Model

All experimental procedures were approved by the Institutional Animal Care and Use Committee at Loma Linda University, Loma Linda, California, USA. All experiments were in concordance with the National Institutes of Health Guide for the Care and Use of Laboratory Animals and the results were reported according to the ARRIVE guidelines.

Adult male Sprague-Dawley rats (450–500 g, Envigo, Indiana, USA) were housed in a humidity and temperature-controlled animal facility with a 12 hour light/dark cycle and ad libitum food and water access. Rat model of asphyxial CA (ACA) was performed with the rats anesthetized deeply with pentobarbital (45 mg/kg, intraperitoneal). Animals were endotracheally intubated under direct laryngoscopy with a 14-gauge plastic catheter. The left femoral artery and vein were then exposed via 1 cm skin incision along the left groin followed by blunt dissection of the surrounding connective tissue. A PE50 catheter (Becton Dickinson, Franklin Lakes, New Jersey, USA) was placed in the femoral artery and was connected to a pressure transducer. Another PE50 catheter was inserted in the left femoral vein for drug administration during resuscitation. Lead-II electrocardiogram was recorded continuously. A rectal probe was inserted to monitor rectal body temperature. Animals were mechanically ventilated (respiratory frequency 100 bpm, tidal volume 0.55 mL/100 g) for 15 minutes before the induction of ACA. ACA was initially induced the initiation of 10 minutes of asphyxia, by disconnecting the ventilator and clamping the intubation tube after chemical neuromuscular blockade with intravenous vecuronium bromide (2 mg/kg). Cardiac arrest was defined as mean arterial pressure <20 mmHg. After 10 minutes of asphyxia, regardless

of the cardiac arrest period, resuscitation was initiated by unclamping the tracheal tube, administering epinephrine (7.5μg/kg) and sodium bicarbonate (1mEq/kg), applying precordial compressions with a pneumatically driven mechanical chest compressor and restarting mechanical ventilation with 100% oxygen at a ratio of 2:1. Thus, the total cardiac arrest period was calculated as the interval between the time at mean arterial pressure < 20 mmHg to the start of CPR. Successful resuscitation and ROSC were defined as mean arterial pressure >60 mmHg and return of spontaneous sinus rhythm for 5 minutes. The animals which did not achieve ROSC or those which achieved ROSC beyond 5 minutes of resuscitation were excluded from the study. Mechanical ventilation was continued with 100% oxygen for 30 minutes post-ROSC and gradually reduced to 21% within 1 hour. Eventually, rats were weaned from the ventilator and extubated. All catheters were withdrawn, the wound was sutured, and the animals were allowed to recover. A heating lamp was used to maintain the body temperature at 36.5±0.5 °C. Respiratory rate, electrocardiogram, end-tidal carbon dioxide and mean arterial pressure were monitored continuously during the whole procedure on a PC-based data-acquisition system supported by WINDAQ software (DATAQ, Akron, Ohio, USA). We did not monitor the oxygen saturations in the current study. Animals in the Sham group underwent the same surgical procedures and baseline ventilation without ACA induction. The baseline and post-ROSC hemodynamics of the rats are presented in Table 1.

Experimental Design—Three main experiments were performed, including time course, outcome and mechanism studies (Fig.1).

Experiment 1: The time course expression of endogenous PAR-2 was evaluated by Western blot at 6, 12, 24 and 72 hours after ACA. Cellular co-localization of PAR-2 with microglia and astrocytes was assessed by double-immunofluorescence staining in Sham and ACA animals at 24 hours following the injury.

Experiment 2: The potential treatment effects of PAR-2 inhibition as well as the detrimental effects of PAR-2 activation on ACA outcomes were examined. Given the lack of a prior literature evidence regarding the optimum dose for the use of selective PAR-2 inhibitor, we have administered 2 different doses of FSLLRY-NH2 (50 μg/rat or 100 μg/rat; Tocris Bioscience, Minneapolis, Minnesota, USA) intranasally at 1 hour post-resuscitation. Selective PAR-2 agonist (AC55541; 30 μg/rat; Santa Cruz Biotechnology, Dallas, Texas, USA) was intranasally administered intranasally at 2 hours post-resuscitation (unpublished data). Short-term neurologic functions were assessed by using the neurological deficit score (NDS), number of seizures and T-maze test over 7 days after ACA. The effects of FSLLRY-NH2 and AC-55541 on hippocampal neuron degeneration were evaluated by Fluoro-Jade C (FJC) staining at 7 days following ACA. Based on better outcomes observed following the administration of FSLLRY-NH2 at a dose of 50 μg, this dose was used for the mechanism study.

Experiment 3: The potential neuroprotective mechanism of PAR-2 inhibition with FSLLRY-NH2 (50 μg/rat) through the inhibition of ERK1/2 phosphorylation and subsequent release of proinflammatory cytokines, was evaluated with Western blot at 24 hours following

ACA. Selective PAR-2 activator AC55541 (30 μg/rat) and ERK1/2 inhibitor PD98059 (Santa Cruz Biotechnology, Dallas, Texas, USA; 2 μl of 2 mmol/L) were used for intervention (25). Neurologic outcome was assessed with the NDS in the mechanism study groups at 24 hours following ACA.

Intranasal Drug Administration

All drugs were diluted in 20% ethanol and delivered via the intranasal route (26). Briefly, rats were placed in supine position under 2% isoflurane anesthesia. Then, a total volume of 36 μL of the (20% ethanol) or 2 different doses of FSLLRY-NH2 (50 μg/rat or 150 μg/rat) were administered at 1 hour after ACA. AC55541 (30 μg/rat) was administered at 2 hours after ACA while PD98059 (2 μl of 2 mmol/L diluted in 34 μl of vehicle to reach the total volume of 36 μL) was administered 30 minutes prior to the induction of ACA. The drugs were administered into the left and right nares, alternating 5 μL into one naris, every 2 minutes for a period of 10 minutes.

Assessment of Neurologic Performance

Neurobehavioral functions were assessed by a blinded investigator. Six parameters including consciousness, respiration, corneal reflex, auditory reflex, motor function, and behavior were evaluated to calculate the *NDS*, at 24 and 48 hours and 7 days after ACA. In this test, higher scores indicated worse performance and the total score of the test ranged between 0 (normal) and 500 (coma) (27, 28). During the first 48 hours after ACA, animals were also closely monitored for a period of 4 hours/day for the *number of seizure* activities (at 24 and 48 hours). Cognitive deficits were evaluated by *T-maze spontaneous alternation test* at 7 days after ACA and the percentage of spontaneous alternation (number of turns in each goal arm) were recorded. The results were expressed as percent with respect to 50% reference (29).

Histological Analyses

Under deep anesthesia, rats underwent a trans-cardiac perfusion of 100 mL of chilled phosphate buffered saline (PBS, 0.01 M, pH 7.4), followed by 100 mL of 10% formalin. The brains were harvested rapidly and fixed in 10% formalin at 4 °C for 24 hours, then dehydrated in 30% sucrose for another 72 hours. After being embedded into OCT (Scigen Scientific Gardena, California, USA), the 10 μm coronal brain sections were obtained at 3.8 mm posterior to the bregma on a cryostat (CM3050S; Leica Microsystems, Bannockburn, III, Germany).

For double-immunofluorescence staining, the slices were washed in 0.01 M of PBS (3×5 minutes) and blocked with 5% donkey serum at room temperature for 1 hour. The slices were then incubated overnight at 4 °C with the following primary antibodies: anti-PAR-2 (1:200), anti-Iba-1 (1:200), anti-GFAP (1:200) (all from Abcam, Cambridge, Massachusetts, USA). On the following day, the sections were incubated with appropriate fluorescence-conjugated secondary antibodies (1:100, Jackson Immuno Research, West Grove, Pennsylvania, USA) at room temperature for 1 hour. The slides were visualized and photographed under a fluorescence microscope (BZ-X800; Keyence Coorporation, Itasca, Illinois, USA) (30, 31).

Fluoro-Jade C Ready-to-Dilute Staining Kit (Biosensis, USA) was used for FJC staining according to the manufacturer's instructions. The number of FJC-positive neurons were counted with ImageJ software (ImageJ 1.5, NIH, USA). The data were presented as the number of FJC-positive neurons as per mm^2 in the fields (26).

Western Blot Analysis

Under deep anesthesia, rats underwent a trans-cardiac perfusion of 100 mL of ice-cold PBS (0.01 M, pH 7.4) before the brains were removed rapidly. Brain samples were snap frozen in liquid nitrogen and stored in −80 °C until use. During preparation, samples were homogenized in RIPA lysis buffer (Santa Cruz Biotechnology Inc., Texas, USA) before centrifuging at 14,000 g at 4 °C for 30 minutes. Protein concentrations of the supernatants were measured using detergent compatible assay (DC protein assay, Bio-Rad Laboratories, California, USA). Equal amounts of protein (30 μg) were separated by SDS-PAGE gel electrophoresis and transferred onto nitrocellulose membranes which were blocked with 5% non-fat blocking grade milk (Bio-Rad, Hercules, California, USA) and incubated overnight at 4 °C with the following primary antibodies: anti-PAR-2 (1:500), anti-ERK1/2 (1:500), anti-p-ERK1/2 (1:500), and anti-β-actin (1:2000) (all from Santa Cruz Biotechnology, Dallas, Texas, USA), anti-IL-6 (1:500) and anti-TNF-α (1:500) (all from Abcam, Cambridge, Massachusetts, USA). On the following day, the membranes were incubated with the appropriate secondary antibody (1:2000, Santa Cruz, Dallas, Texas, USA) at room temperature for 2 hours. The bands were visualized with ECL Plus chemiluminescence reagent kit (Amersham Bioscience, Pennsylvania, USA). The immunoblot densities were quantified using the ImageJ software (Image J 1.4, NIH, USA). β-actin was used as internal control (32).

Statistical Analysis

All data were presented as the mean and standard deviation (mean ± SD) and analyzed using GraphPad Prism 7 (GraphPad Software, San Diego, California, USA). One-way ANOVA followed by Tukey's post hoc test was used for comparison among multiple groups. Log-rank test was used for comparing survival distribution between groups. $p<0.05$ was considered statistically significant.

Results

Characteristics of the Asphyxial Cardiac Arrest Rat Model and Mortality

A total of 116 rats were randomly divided into Sham (n= 18) and ACA (n= 98) groups. ROSC was achieved in 71 (72.5%) of the 98 rats that were subjected to ACA. Only the resuscitated rats which achieved ROSC (n=71) were included for our experimental studies. Five of the animals which achieved ROSC died during the study period (Post-ROSC mortality, 7%). There was no significant difference in the mortality rates among ACA groups ($p=0.7075$).

The baseline as well as post-resuscitation hemodynamics of the subjects are summarized in Table-1. During the ACA rat model, each animal was subjected to 10-minutes asphyxia. Accordingly, the cardiac arrest period as well as cardiopulmonary resuscitation time differed

between animals. The mean time from the initiation of asphyxia to the reach of pulseless electricity (MAP ≤ 20 mmHg) was 256 ± 21.12 seconds, thus resulting in a mean cardiac arrest period of 344 ± 21 seconds. There was no significant difference of either time to cardiac arrest or arrest period among groups (data not shown).

Temporal expression of endogenous PAR-2 in the brain after ACA

Western blot analysis showed that PAR-2 levels were significantly increased as early as 6 hours after ACA, peaked at 24 hours and the elevation was sustained until 72 hours compared to the Sham group (Fig. 2A).

Double-immunofluorescence staining of PAR-2 with calcium-binding adaptor molecule 1 (Iba-1, a marker for microglia) and glial fibrillary acidic protein (GFAP, a marker for astrocytes) revealed that PAR-2 was expressed in microglia and astrocytes both in Sham and ACA animals at 24 hours following ACA. There were more PAR-2-positive microglia and astrocytes in the ACA group compared to the Sham group (Fig. 2B).

Inhibition of PAR-2 attenuated neurobehavioral impairment following ACA

ACA resulted in significant neurological impairment compared to the Sham group, as defined by the higher NDS and higher number of seizures at 24 and 48 hours, as well as the lower spontaneous alteration in the T-maze test at 7 days after ACA. Treatment with FSLLRY-NH2 at a dose of 50 μg significantly improved performance in all tests and at all time points compared to vehicle treated ACA rats. FSLLRY-NH2 treatment at a dose of 100 μg effectively improved neurologic outcomes as well; however, no significant difference was reached in NDS at 24 hours and the T-maze test at 7 days after ACA. Consistently, the administration of PAR-2 agonist AC55541 markedly worsened NDS and T-maze performance and increased the number of seizures compared to the ACA + vehicle group (Fig. 3A–C).

Inhibition of PAR-2 reduced hippocampal neuronal degeneration at 7 days following ACA

Fluoro-Jade C staining revealed that ACA markedly increased neuronal degeneration within the hippocampal CA1 region at 7 days after ACA. Compared to the ACA + vehicle group, the inhibition of PAR-2 with FSLLRY-NH2 at both doses of 50 μg and 100 μg significantly reduced the number of FJC-positive neurons within the hippocampal CA1 region while activation of PAR-2 with AC55541 significantly enhanced the number of degenerating cells (Fig. 4A, B).

Inhibition of PAR-2 showed anti-neuroinflammatory effect by suppressing the phosphorylation of ERK1/2

Western blotting was performed to evaluate the potential mechanism of neuroprotection provided by PAR-2 inhibition at 24 hours after ACA. The results showed that the expression of PAR-2, p-ERK1/2 as well as proinflammatory cytokines TNF-α and IL-6 were significantly increased, while ERK1/2 levels did not change at 24 hours after ACA compared with the Sham group. Treatment with FSLLRY-NH2 significantly reduced PAR-2, p-ERK1/2, TNF-α and IL-6 levels compared to the vehicle treated ACA group. On the other hand, further activation of PAR-2 with AC55541 aggravated the neuroinflammatory

response by increasing the protein levels of p-ERK1/2. This proinflammatory effect of AC55541 was abolished by the administration of potent ERK1/2 inhibitor PD98059, confirming p-ERK1/2 as the downstream effector of PAR-2 mediated neuroinflammation following ACA (Fig. 5A–F).

Inhibition of ERK1/2 reversed the detrimental effect of PAR-2 activation on neurologic function following ACA

The inhibition of PAR-2 with FSLLRY-NH2 significantly improved the NDS compared to the ACA + vehicle group at 24 hours following ACA. Further activation of PAR-2 with AC55541 markedly deteriorated neurological performance compared to the ACA + vehicle group, which was offset by the ERK1/2 inhibitor, PD98059 (Fig. 5G).

Discussion

Using a rat model of ACA, we found that GCI and reperfusion increased PAR-2 expression in the brain and was associated with poor neurobehavioral performance, higher protein level of p-ERK1/2 and proinflammatory cytokines of IL-6 and TNF-α, and more hippocampal CA1 neuron degeneration in resuscitated rats. Consistently, the inhibition of PAR-2 reduced neuroinflammation and improved the neurological functions by suppressing ERK1/2 phosphorylation. On the other hand, PAR-2 agonist further aggravated the CA induced neuroinflammatory response leading to more neuronal degeneration in the hippocampal CA1 region and deteriorated neurological impairment caused by ACA.

Tryptase, which is known to potentiate the release of proinflammatory cytokines from the peripheral immune cells (33), microglia (20) and astrocytes (21), is the major secretory protein of mast cells. The activator effect of tryptase on microglia and astrocytes was mediated through the activation of PAR-2 and resulted in the release of IL-6 and TNF-α in earlier *in-vitro* studies (20, 21). PAR-2, the endogenous receptor for tryptase is a unique member of the PAR family as the other members (PAR-1, 3 and 4) are activated by thrombin (17). Increased expression and activation of PAR-2 have been implicated in neuroinflammation and neurodegeneration (34–36). Similarly, following ischemic brain injury, upregulated expression of PAR-2 was previously demonstrated both *in-vivo* and *in-vitro* (37–39). In addition to its contribution to the activation of microglia and astrocytes during neuroinflammation, the activation of PAR-2 also resulted in neuronal cell death and disruption of the blood brain barrier (16, 40, 41). During the tryptase mediated neuroinflammatory response, PAR-2 led to the activation of mitogen-activated protein kinases (MAPK) and nuclear factor kappa-B (NFkB) signaling pathways that are involved in the generation of proinflammatory cytokines (15, 20). Interestingly, PAR-2 mediated the I/R injury following its activation by tryptase in organs other than the brain such as the lungs (42) and small intestines (43) as well. In addition, some studies have suggested a neuroprotective role of PAR-2 by activating neuronal ERK1/2 signaling and triggering reactive astroglial activation under ischemic conditions (44), which was considered pathological by some others (9). Nonetheless, the controversial results obtained from the abovementioned studies evaluating the contribution of PAR-2 to ischemic brain injury could have resulted from the variations in the functional role of PAR-2 in different cell types and

in different kinds of injury mechanisms. In fact, consistent with previous works showing the contribution of mast cell-derived tryptase to ischemic brain injury (45), we recently observed elevated levels of tryptase in the brain following CA in rats. Moreover, inhibition of tryptase, the endogenous PAR-2 ligand, attenuated hippocampal neuronal degeneration and led to improved neurocognitive functions by diminishing neuroinflammation which was mediated by PAR-2 and its downstream effectors p38 MAPK and NFkB signaling pathways (unpublished data). In the present study, we have focused on the potential neuroprotective role of the inhibition of PAR-2 mediated neuroinflammation at the receptor level.

Inhibition of the neuroinflammatory response following GCI is known to reduce I/R induced hippocampal neuronal death and learning and memory deficits (46). Evidence from both clinical human studies and experimental research has pointed to the role of mast cells in neuroinflammation associated cognitive dysfunction (47, 48). However, despite emerging evidence underlining the intercourse between mast cell-derived tryptase and PAR-2 in the regulation of neuroinflammation, little research has focused on the involvement of PAR-2 in such neurocognitive decline so far. Additionally, although a potential protective role of neuronal PAR-2 was previously suggested in neuroinflammation associated cognitive impairment (49), a negative regulatory role of PAR-2 activation on learning and memory was reported afterwards (50). In line with previous evidence underlining the contribution of PAR-2 to neuroinflammation associated conditions, in the present study, we demonstrated less hippocampal neuronal degeneration and improved short-term neurocognitive functions by inhibiting the ACA-induced activation of PAR-2 and the benefit observed in T-maze neurocognitive performance correlated with the extinguished neuroinflammatory condition.

Increased activation of ERK1/2 persisting up to 24 hours post-ROSC was reported in previous ACA models (24). Moreover, inhibition of ERK1/2 signaling by prohibiting its phosphorylation was associated with improved survival rates and better neurologic outcomes (24). Earlier studies also reported that ERK1/2 was one of the MAPK involved in the activation of microglia and astrocytes and subsequent release of proinflammatory cytokines through the activation of PAR-2 (20, 21). Consistently, we observed increased expression of p-ERK1/2 together with enhanced levels of proinflammatory cytokines in the brain following ACA. Moreover, augmented phosphorylation and thus, activation of ERK1/2 was due to the increased expression and activation of PAR-2 in the ischemic brain such that inhibition of PAR-2 with FSLLRY-NH2 attenuated p-ERK1/2 levels. Conversely, activation of PAR-2 by exogenous PAR-2 agonist resulted in further increase in the protein levels of PAR-2 and p-ERK1/2, IL-6 and TNF-α. In our study, the augmented release of proinflammatory cytokines in response to overexpression of PAR-2 with AC55541 was abolished by the administration of ERK1/2 inhibitor PD98059, which suggested that p-ERK1/2 was the downstream effector of PAR-2 in the mediation of CA induced neuroinflammation. Neurologic deficits were associated with the status of the neuroinflammation since FSLLRY-NH2 significantly improved the NDS which was markedly worsened with AC55541 alone at 24 hours following ACA. Consistently, this detrimental effect of AC55541 on neurological function was also offset by PD98059.

Collectively, our results show the deleterious effects of PAR-2 mediated neuroinflammation on hippocampal neuronal degeneration and associated neurocognitive decline after ACA.

The neuroprotection provided by the inhibition of PAR-2 was at least partly mediated through the ERK1/2 signaling pathway. However, it remains to be determined if other mechanisms such as the blood brain barrier preservation or anti-neuronal apoptosis also contribute to the neuroprotection provided by PAR-2 inhibition.

Conclusions

Inhibition of PAR-2 prevents CA associated short-term hippocampal neuronal degeneration and neurocognitive dysfunction by attenuating neuroinflammation in a rat model of ACA. Thus, targeting the PAR-2 mediated neuroinflammatory response remains a promising therapeutic strategy to improve post-CA neurocognitive decline.

Acknowledgements

Funding

This research was supported by the National Institutes of Health, Grant/Award Number: P01NS082184 and Loma Linda University Neurosurgery Department Research Fund (IACUC Record Number: 8180029).

Abbreviations

ACA	Asphyxial CA
CA	Cardiac arrest
FJC	Fluoro-Jade C
GCI	Global cerebral ischemia
GFAP	Glial fibrillary acidic protein
Iba-1	Calcium-binding adaptor molecule 1
I/R	Ischemia/reperfusion
MAPK	Mitogen-activated protein kinases
NDS	Neurological deficit score
NFkB	Nuclear factor kappa-B
PBS	Phosphate buffered saline
PAR-2	Protease activated receptor-2
ROSC	return of spontaneous circulation

References

1. Field JM, Hazinski MF, Sayre MR, Chameides L, Schexnayder SM, Hemphill R, Samson RA, Kattwinkel J, Berg RA, Bhanji F, et al.: Part 1: executive summary: 2010 American Heart Association Guidelines for Cardiopulmonary Resuscitation and Emergency Cardiovascular Care. Circulation 122(18 Suppl 3):S640–656, 2010. [PubMed: 20956217]

2. Nolan JP, Neumar RW, Adrie C, Aibiki M, Berg RA, Bottiger BW, Callaway C, Clark RS, Geocadin RG, Jauch EC, et al.: Post-cardiac arrest syndrome: epidemiology, pathophysiology, treatment, and prognostication. A Scientific Statement from the International Liaison Committee on Resuscitation; the American Heart Association Emergency Cardiovascular Care Committee; the Council on Cardiovascular Surgery and Anesthesia; the Council on Cardiopulmonary, Perioperative, and Critical Care; the Council on Clinical Cardiology; the Council on Stroke. Resuscitation 79(3):350–379, 2008. [PubMed: 18963350]

3. Laver S, Farrow C, Turner D, Nolan J: Mode of death after admission to an intensive care unit following cardiac arrest. Intensive Care Med 30(11):2126–2128, 2004. [PubMed: 15365608]

4. Greer DM: Mechanisms of injury in hypoxic-ischemic encephalopathy: implications to therapy. Semin Neurol 26(4):373–379, 2006. [PubMed: 16969737]

5. Sugawara T, Lewen A, Noshita N, Gasche Y, Chan PH: Effects of global ischemia duration on neuronal, astroglial, oligodendroglial, and microglial reactions in the vulnerable hippocampal CA1 subregion in rats. J Neurotrauma 19(1):85–98, 2002. [PubMed: 11852981]

6. Yigitkanli K, Zheng Y, Pekcec A, Lo EH, van Leyen K: Increased 12/15-Lipoxygenase Leads to Widespread Brain Injury Following Global Cerebral Ischemia. Transl Stroke Res 8(2):194–202, 2017. [PubMed: 27838820]

7. Stamenova V, Nicola R, Aharon-Peretz J, Goldsher D, Kapeliovich M, Gilboa A: Long-term effects of brief hypoxia due to cardiac arrest: Hippocampal reductions and memory deficits. Resuscitation 126:65–71, 2018. [PubMed: 29474878]

8. Amantea D, Nappi G, Bernardi G, Bagetta G, Corasaniti MT: Post-ischemic brain damage: pathophysiology and role of inflammatory mediators. FEBS J 276(1):13–26, 2009. [PubMed: 19087196]

9. Wan YJ, Xu L, Song WT, Liu YQ, Wang LC, Zhao MB, Jiang Y, Liu LY, Zeng KW, Tu PF: The Ethanolic Extract of Caesalpinia sappan Heartwood Inhibits Cerebral Ischemia/Reperfusion Injury in a Rat Model Through a Multi-Targeted Pharmacological Mechanism. Front Pharmacol 10:29, 2019. [PubMed: 30804781]

10. Gutierrez-Vargas JA, Munera A, Cardona-Gomez GP: CDK5 knockdown prevents hippocampal degeneration and cognitive dysfunction produced by cerebral ischemia. J Cereb Blood Flow Metab 35(12):1937–1949, 2015. [PubMed: 26104286]

11. Lim C, Alexander MP, LaFleche G, Schnyer DM, Verfaellie M: The neurological and cognitive sequelae of cardiac arrest. Neurology 63(10):1774–1778, 2004. [PubMed: 15557489]

12. Frisch S, Thiel F, Schroeter ML, Jentzsch RT: Apathy and Cognitive Deficits in Patients with Transient Global Ischemia After Cardiac Arrest. Cogn Behav Neurol 30(4):172–175, 2017. [PubMed: 29256912]

13. Buanes EA, Gramstad A, Sovig KK, Hufthammer KO, Flaatten H, Husby T, Langorgen J, Heltne JK: Cognitive function and health-related quality of life four years after cardiac arrest. Resuscitation 89:13–18, 2015. [PubMed: 25596374]

14. Roine RO, Kajaste S, Kaste M: Neuropsychological sequelae of cardiac arrest. JAMA 269(2):237–242, 1993. [PubMed: 8417242]

15. Luo W, Wang Y, Reiser G: Protease-activated receptors in the brain: receptor expression, activation, and functions in neurodegeneration and neuroprotection. Brain Res Rev 56(2):331–345, 2007. [PubMed: 17915333]

16. Zhou Q, Wang YW, Ni PF, Chen YN, Dong HQ, Qian YN: Effect of tryptase on mouse brain microvascular endothelial cells via protease-activated receptor 2. J Neuroinflammation 15(1):248, 2018. [PubMed: 30170602]

17. Ossovskaya VS, Bunnett NW: Protease-activated receptors: contribution to physiology and disease. Physiol Rev 84(2):579–621, 2004. [PubMed: 15044683]

18. Hendriksen E, van Bergeijk D, Oosting RS, Redegeld FA: Mast cells in neuroinflammation and brain disorders. Neurosci Biobehav Rev 79:119–133, 2017. [PubMed: 28499503]

19. Ocak U, Ocak PE, Wang A, Zhang JH, Boling W, Wu P, Mo J, Zhang T, Huang L: Targeting mast cell as a neuroprotective strategy. Brain Inj 33(6):723–733, 2019. [PubMed: 30554528]

20. Zhang S, Zeng X, Yang H, Hu G, He S: Mast cell tryptase induces microglia activation via protease-activated receptor 2 signaling. Cell Physiol Biochem 29(5–6):931–940, 2012. [PubMed: 22613992]
21. Zeng X, Zhang S, Xu L, Yang H, He S: Activation of protease-activated receptor 2-mediated signaling by mast cell tryptase modulates cytokine production in primary cultured astrocytes. Mediators Inflamm 2013:140812, 2013. [PubMed: 23818741]
22. Alessandrini A, Namura S, Moskowitz MA, Bonventre JV: MEK1 protein kinase inhibition protects against damage resulting from focal cerebral ischemia. Proc Natl Acad Sci U S A 96(22):12866–12869, 1999. [PubMed: 10536014]
23. Hu BR, Liu CL, Park DJ: Alteration of MAP kinase pathways after transient forebrain ischemia. J Cereb Blood Flow Metab 20(7):1089–1095, 2000. [PubMed: 10908042]
24. Nguyen Thi PA, Chen MH, Li N, Zhuo XJ, Xie L: PD98059 Protects Brain against Cells Death Resulting from ROS/ERK Activation in a Cardiac Arrest Rat Model. Oxid Med Cell Longev 2016:3723762, 2016. [PubMed: 27069530]
25. Wang J, Zhang S, Ma H, Yang S, Liu Z, Wu X, Wang S, Zhang Y, Liu Y: Chronic Intermittent Hypobaric Hypoxia Pretreatment Ameliorates Ischemia-Induced Cognitive Dysfunction Through Activation of ERK1/2-CREB-BDNF Pathway in Anesthetized Mice. Neurochem Res 42(2):501–512, 2017. [PubMed: 27822668]
26. Mo J, Enkhjargal B, Travis ZD, Zhou K, Wu P, Zhang G, Zhu Q, Zhang T, Peng J, Xu W, et al.: AVE 0991 attenuates oxidative stress and neuronal apoptosis via Mas/PKA/CREB/UCP-2 pathway after subarachnoid hemorrhage in rats. Redox Biol 20:75–86, 2019. [PubMed: 30296700]
27. Hendrickx HH, Rao GR, Safar P, Gisvold SE: Asphyxia, cardiac arrest and resuscitation in rats. I. Short term recovery. Resuscitation 12(2):97–116, 1984. [PubMed: 6091205]
28. Huang L, Applegate RL II, Applegate PM, Gong L, Ocak U, Boling W, Zhang JH: Inhalation of high-concentration hydrogen gas attenuates cognitive deficits in a rat model of asphyxia induced-cardiac arrest. Med Gas Res 9(3):122–126, 2019. [PubMed: 31552874]
29. Matchett GA, Calinisan JB, Matchett GC, Martin RD, Zhang JH: The effect of granulocyte-colony stimulating factor in global cerebral ischemia in rats. Brain Res 1136(1):200–207, 2007. [PubMed: 17210148]
30. Li P, Zhao G, Ding Y, Wang T, Flores J, Ocak U, Wu P, Zhang T, Mo J, Zhang JH, et al.: Rh-IFN-alpha attenuates neuroinflammation and improves neurological function by inhibiting NF-kappaB through JAK1-STAT1/TRAF3 pathway in an experimental GMH rat model. Brain Behav Immun 79:174–185, 2019. [PubMed: 30711510]
31. Zuo Y, Huang L, Enkhjargal B, Xu W, Umut O, Travis ZD, Zhang G, Tang J, Liu F, Zhang JH: Activation of retinoid X receptor by bexarotene attenuates neuroinflammation via PPARgamma/SIRT6/FoxO3a pathway after subarachnoid hemorrhage in rats. J Neuroinflammation 16(1):47, 2019. [PubMed: 30791908]
32. Zhang T, Xu S, Wu P, Zhou K, Wu L, Xie Z, Xu W, Luo X, Li P, Ocak U, et al.: Mitoquinone attenuates blood-brain barrier disruption through Nrf2/PHB2/OPA1 pathway after subarachnoid hemorrhage in rats. Exp Neurol 317:1–9, 2019. [PubMed: 30779914]
33. Malamud V, Vaaknin A, Abramsky O, Mor M, Burgess LE, Ben-Yehudah A, Lorberboum-Galski H: Tryptase activates peripheral blood mononuclear cells causing the synthesis and release of TNF-alpha, IL-6 and IL-1 beta: possible relevance to multiple sclerosis. J Neuroimmunol 138(1–2):115–122, 2003. [PubMed: 12742661]
34. Liu P, Sun L, Zhao XL, Zhang P, Zhao XM, Zhang J: PAR2-mediated epigenetic upregulation of alpha-synuclein contributes to the pathogenesis of Parkinsons disease. Brain Res 1565:82–89, 2014. [PubMed: 24747612]
35. Smith-Swintosky VL, Cheo-Isaacs CT, D'Andrea MR, Santulli RJ, Darrow AL, Andrade-Gordon P: Protease-activated receptor-2 (PAR-2) is present in the rat hippocampus and is associated with neurodegeneration. J Neurochem 69(5):1890–1896, 1997. [PubMed: 9349532]
36. Kempuraj D, Selvakumar GP, Thangavel R, Ahmed ME, Zaheer S, Kumar KK, Yelam A, Kaur H, Dubova I, Raikwar SP, et al.: Glia Maturation Factor and Mast Cell-Dependent Expression of Inflammatory Mediators and Proteinase Activated Receptor-2 in Neuroinflammation. J Alzheimers Dis 66(3):1117–1129, 2018. [PubMed: 30372685]

37. Striggow F, Riek-Burchardt M, Kiesel A, Schmidt W, Henrich-Noack P, Breder J, Krug M, Reymann KG, Reiser G: Four different types of protease-activated receptors are widely expressed in the brain and are up-regulated in hippocampus by severe ischemia. Eur J Neurosci 14(4):595–608, 2001. [PubMed: 11556885]
38. Morihara R, Yamashita T, Kono S, Shang J, Nakano Y, Sato K, Hishikawa N, Ohta Y, Heitmeier S, Perzborn E, et al.: Reduction of intracerebral hemorrhage by rivaroxaban after tPA thrombolysis is associated with downregulation of PAR-1 and PAR-2. J Neurosci Res 95(9):1818–1828, 2017. [PubMed: 28035779]
39. Ocak U, Ocak Eser P, Huang L, Zhang JH: FSLLRY-NH2 Improves Neurological Outcome After Cardiac Arrest in Rats. Turk Neurosurg, 2019.
40. Park GH, Jeon SJ, Ko HM, Ryu JR, Lee JM, Kim HY, Han SH, Kang YS, Park SH, Shin CY, et al.: Activation of microglial cells via protease-activated receptor 2 mediates neuronal cell death in cultured rat primary neuron. Nitric Oxide 22(1):18–29, 2010. [PubMed: 19887113]
41. Domotor E, Bartha K, Machovich R, Adam-Vizi V: Protease-activated receptor-2 (PAR-2) in brain microvascular endothelium and its regulation by plasmin and elastase. J Neurochem 80(5):746–754, 2002. [PubMed: 11948237]
42. Gan X, Liu D, Huang P, Gao W, Chen X, Hei Z: Mast-cell-releasing tryptase triggers acute lung injury induced by small intestinal ischemia-reperfusion by activating PAR-2 in rats. Inflammation 35(3):1144–1153, 2012. [PubMed: 22200983]
43. Liu D, Gan X, Huang P, Chen X, Ge M, Hei Z: Inhibiting tryptase after ischemia limits small intestinal ischemia-reperfusion injury through protease-activated receptor 2 in rats. J Trauma Acute Care Surg 73(5):1138–1144, 2012. [PubMed: 22976423]
44. Jin G, Hayashi T, Kawagoe J, Takizawa T, Nagata T, Nagano I, Syoji M, Abe K: Deficiency of PAR-2 gene increases acute focal ischemic brain injury. J Cereb Blood Flow Metab 25(3):302–313, 2005. [PubMed: 15647743]
45. McKittrick CM, Lawrence CE, Carswell HV: Mast cells promote blood brain barrier breakdown and neutrophil infiltration in a mouse model of focal cerebral ischemia. J Cereb Blood Flow Metab 35(4):638–647, 2015. [PubMed: 25564235]
46. Chu K, Yin B, Wang J, Peng G, Liang H, Xu Z, Du Y, Fang M, Xia Q, Luo B: Inhibition of P2X7 receptor ameliorates transient global cerebral ischemia/reperfusion injury via modulating inflammatory responses in the rat hippocampus. J Neuroinflammation 9:69, 2012. [PubMed: 22513224]
47. Zhang X, Dong H, Li N, Zhang S, Sun J, Zhang S, Qian Y: Activated brain mast cells contribute to postoperative cognitive dysfunction by evoking microglia activation and neuronal apoptosis. J Neuroinflammation 13(1):127, 2016. [PubMed: 27245661]
48. Piette F, Belmin J, Vincent H, Schmidt N, Pariel S, Verny M, Marquis C, Mely J, Hugonot-Diener L, Kinet JP, et al.: Masitinib as an adjunct therapy for mild-to-moderate Alzheimer's disease: a randomised, placebo-controlled phase 2 trial. Alzheimers Res Ther 3(2):16, 2011. [PubMed: 21504563]
49. Noorbakhsh F, Vergnolle N, McArthur JC, Silva C, Vodjgani M, Andrade-Gordon P, Hollenberg MD, Power C: Proteinase-activated receptor-2 induction by neuroinflammation prevents neuronal death during HIV infection. J Immunol 174(11):7320–7329, 2005. [PubMed: 15905579]
50. Lohman RJ, Jones NC, O'Brien TJ, Cocks TM: A regulatory role for protease-activated receptor-2 in motivational learning in rats. Neurobiol Learn Mem 92(3):301–309, 2009. [PubMed: 19410009]

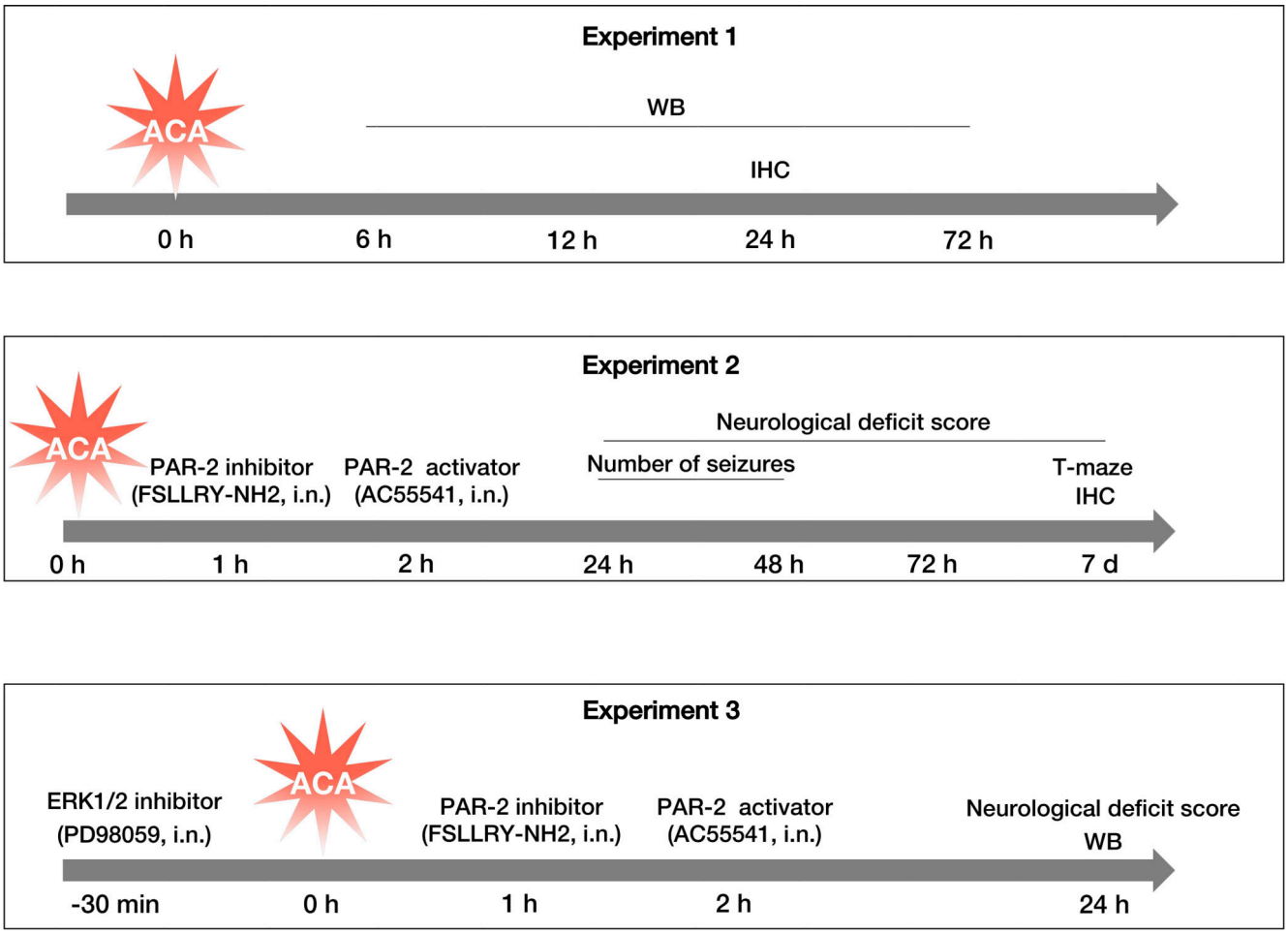

Fig. 1:

Experimental design for the present study.

Three main experiments included time course study (experiment 1), short-term outcome study (experiment 2), and mechanism study (experiment 3).

d: days, **h:** hours, **IHC:** immunohistochemistry, **i.n:** intranasal, **min:** minutes, **WB:** Western blot.

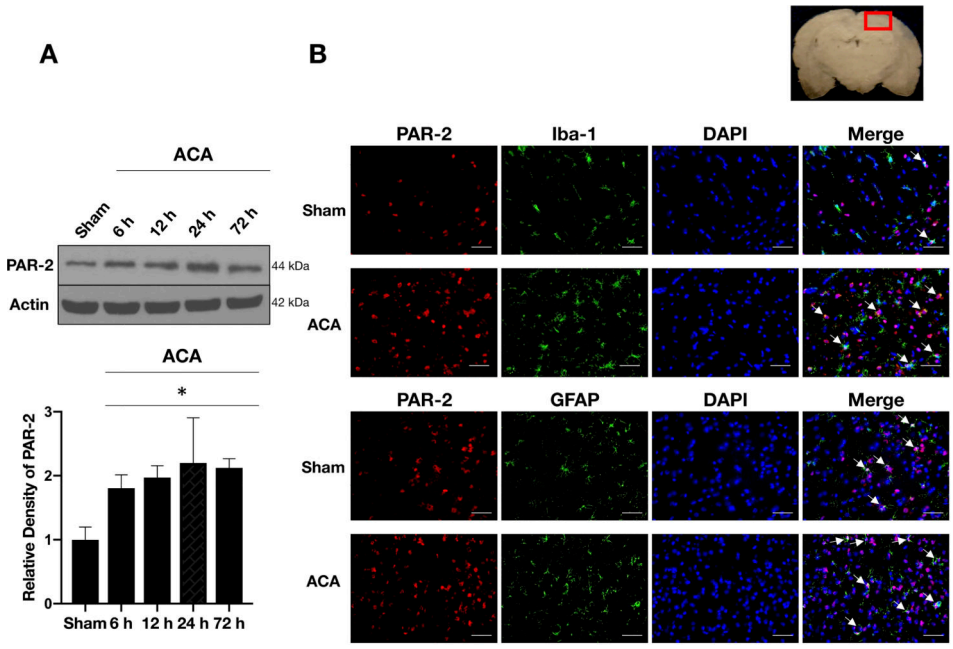

Fig. 2:

Time course expression of endogenous PAR-2 following ACA.

A) Representative Western blot images and quantitative analyses of endogenous PAR-2 over 72 hours following ACA showed significantly increased expression of PAR-2 which started at 6 hours following ACA and remained high up to 72 hours compared to the shams. Data are expressed as mean ± SD. n= 4/group. ANOVA, Tukey. *p<0.05 compared to Sham group.

B) Representative microphotographs of double-immunofluorescence staining of PAR-2 with microglia (Iba-1) and astrocytes (GFAP) showed that PAR-2 (red) co-localized with Iba-1-positive microglia (green) and GFAP-positive astrocytes (green) in both Sham and ACA groups (white arrows). Top panel indicates the location of staining (small red box). Scale bar= 50 μm, n= 2/group.

ACA: asphyxial cardiac arrest, **GFAP:** glial fibrillary acidic protein, **h:** hours, **Iba-1:** calcium-binding adaptor molecule 1.

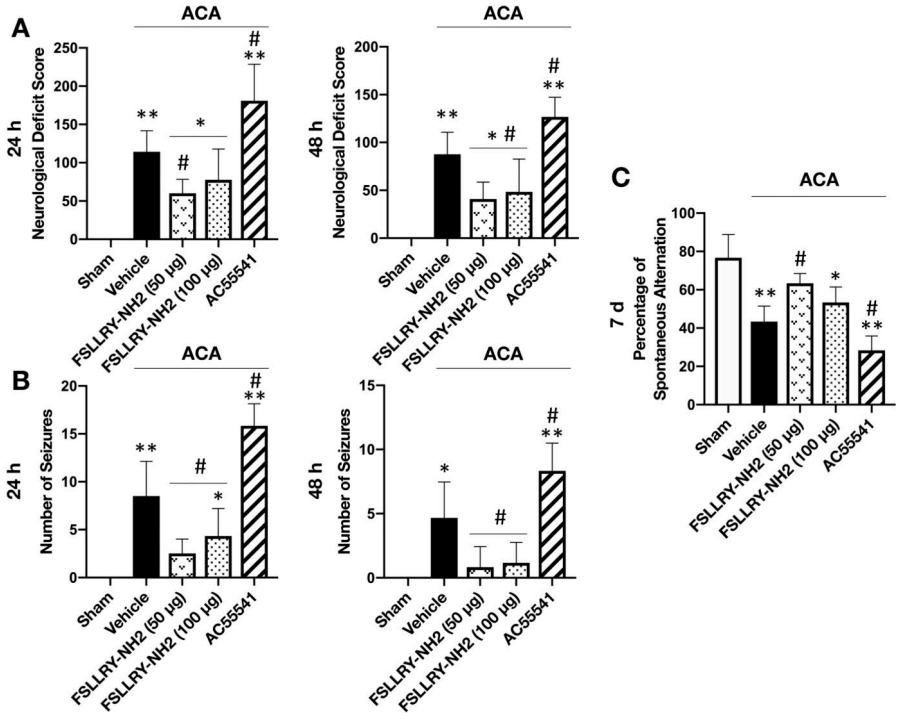

Fig. 3:

Effect of FSLLRY-NH2 on neurocognitive functions after ACA.

Effect of FSLLRY-NH2 on neurological functions were assessed by (A) NDS at 24 and 48 hours, (B) number of seizures at 24 and 48 hours and (C) T-maze test at 7 days after ACA. ACA significantly worsened performance while treatment with FSLLRY-NH2 at a dose of 50 µg significantly improved neurological functions in all tests following ACA. FSLLRY-NH2 treatment at a dose of 100 µg was not effective in NDS at 24 hours and T-maze test. AC55541 significantly deteriorated neurobehavioral outcome at all time points compared to the vehicle treated ACA group. Data are expressed as mean ± SD. n= 6/group. ANOVA, Tukey. ** $p<0.001$ vs. Sham group, * $p<0.05$ vs. Sham group, # $p<0.05$ vs. ACA + vehicle group.

ACA: Asphyxial cardiac arrest, **d:** days, **h:** hours.

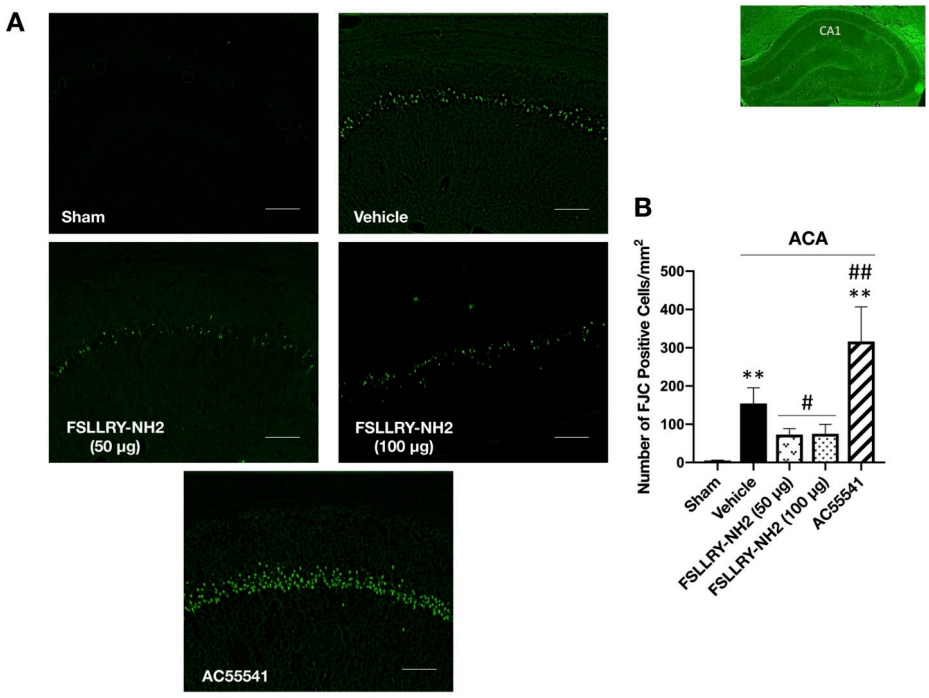

Fig. 4:

Effect of FSLLRY-NH2 on neuronal degeneration after ACA.

Representative microphotographs (A) and quantitative analyses (B) of FJC-positive cells revealed significant neuronal degeneration in hippocampal CA1 region at 7 days after ACA. AC55541 further exacerbated the number of FJC-positive cells in rats subjected to ACA while FSLLRY-NH2 at doses of 50 µg and 150 µg markedly reduced hippocampal neuronal degeneration. Data are expressed as mean ± SD. n= 6/group. ANOVA, Tukey. Scale bar= 100 µm. ** p<0.001 vs. Sham group, ## p<0.001 vs. ACA + vehicle group, # p<0.05 vs. ACA + vehicle group.

ACA: asphyxial cardiac arrest

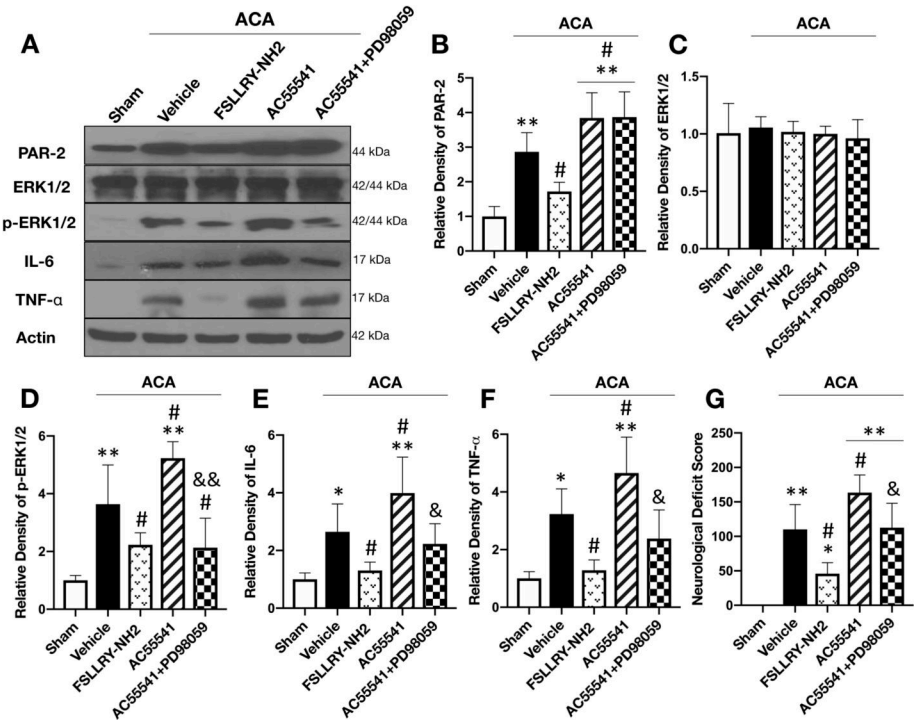

Fig. 5:

Inhibition of ERK1/2 abolished the neuroinflammatory effect of PAR-2 activation at 24 hours after ACA.

Representative Western blot images (A) and quantitative analysis of PAR-2 (B), ERK1/2 (C), p-ERK1/2 (D), IL-6 (E) and TNF- α (F) in the brain revealed increased protein levels at 24 hours following ACA except for ERK1/2 compared to the Sham group. Treatment with FSLLRY-NH2 significantly reduced p-ERK1/2 and proinflammatory cytokine levels compared to the ACA + vehicle group. Further activation of PAR-2 with AC55541 only aggravated the neuroinflammatory response by increasing p-ERK1/2 expression. Potent ERK1/2 inhibitor PD98059 reversed the neuroinflammatory effect of AC55541. Neurologic outcome assessment with NDS at 24 hours following ACA (G) revealed that the inhibition of PAR-2 significantly improved neurologic function while AC55541 alone significantly worsened performance compared to the ACA + vehicle group. This detrimental effect of AC55541 on NDS was reversed by the ERK1/2 inhibitor, PD98059. Data are expressed as mean ± SD. n= 6/group. ANOVA, Tukey. $^{**}p<0.001$ vs. Sham group, $^{*}p<0.05$ vs. Sham group, $\#p<0.05$ vs. ACA + vehicle group, $\&\&p<0.001$ compared to ACA + AC55541 group, $\&p<0.05$ compared to ACA + AC55541 group.

ACA: asphyxial cardiac arrest

Table 1:

Baseline and post-resuscitation hemodynamics and the resuscitation time of the animals.

Parameters	Baseline	Post-ROSC 5 min	Post-ROSC 30 min	Post-ROSC 60 min
Body weight (g)	451.4 (± 22.6)	-	-	-
MAP (mmHg)	118.3 (± 8.6)	101.2 (± 9)	104 (± 10.2)	112.4 (± 10.7)
Hearth rate (beats/minute)	377 (± 25.2)	380 (± 12.9)	388.1 (± 14.6)	386.2 (± 28.5)
EtCO2 (mmHg)	47 (± 4.6)	55.5 (± 5.1)	52.8 (± 2.7)	52.4 (± 4.2)
Time to ACA (MAP < 20 mmHg)	256 (± 21.1)	-	-	-
Cardiac Arrest Period (seconds)	344 (± 21)	-	-	-
CPR time (seconds)	119.9 (± 47.3)	-	-	-

Data are expressed as mean ± standard deviation. A**CA:** Asphyxial cardiac arrest, **CPR:** Cardiopulmonary resuscitation, **EtCO2:** End-tidal carbon dioxide, **MAP:** Mean arterial pressure, **ROSC:** Return of spontaneous circulation